ANALYTICAL SCIENCE & TECHNOLOGY
(Journal of the Korean Society of Analytical Sciences)
Vol. 8, No. 4, 1995
Printed in the Republic of Korea

Preparation and Characterization of Doped Fe_2O_3 and GaAs Photosemiconductive Electrodes for CO_2 Fixation

Il Kwang Kim*, Seong Jae Lee, Min Su Kim, Seung Il Jeong, Byung Sun Park+, and Youn Geun Kim++

**Department of Chemistry, Wonkwang University, Iksan City, 570-749, Korea*
+Electronics and Telecommunications Research Institute, Taejon, 305-606, Korea
++Itaya Electrochem. Lab., Dohoku University, Sendai, 982, Japan
(Received August 20, 1995)

Abstract : The preparation and characterization of photosemiconductive electrodes of GaAs and of Fe_2O_3 doped with MgO or CaO were investigated. The doped Fe_2O_3 photosemiconductive electrodes were prepared from thin films sintered at temperatures from 1,100 to 1,450℃, and rapidly quenched in distilled water. The surfaces of the electrodes containing both corundum structure of Fe_2O_3 and spinel structure of $Mg_xFe_{3-x}O_4$ or $Ca_xFe_{3-x}O_4$ were analyzed by X-ray diffraction and scanning electron microscopy. The cathodic and anodic photocurrents on these electrodes indicated a critical doping amount of 5-11 wt. %. The photocurrents were enhanced when GaAs electrodes were treated with methylene violet the anodic photocurrents were temporarial enhanced and changed to the cathodic ptotocurrents after the surface was dryed.

Keywords : Iron oxide, photoelectrochemistry, thin film, GaAs

Introduction

The photoelectrolysis of water by photosemiconductors has received considerable attention as an alternative means of using solar energy. Since Fujishima and Honda[1] first reported the photodissociation of water by TiO_2 electrodes, Gerischer[2] has developed a theoretical basis for semiconductor photoelectrolysis. In particular, iron oxide(α -Fe_2O_3) has received remarkable attention due

to its many desirable qualities such as low price and small bandgap[3-5] as well as the possible application to photoelectrochemical cells for the dissociation of water. It has a bandgap of 2.3 eV which permits the use of about 40% of the incident solar radiation. It is abundant, inexpensive and stable in various aqueous solutions with a broad pH range. However, an external potential was needed in conjunction with illumination when using pure α-Fe_2O_3 in order to produce hydrogen and oxygen from water. Various methods to eliminate the need to use an external potential have been explored [6-9]. Gardner *et al.* [10,11] have reported that *p*-type(photocathode) photocurrents were generated from Mg, or Ca-doped Fe_2O_3 when the electrodes were sintered at high temperatures. This cathodic photocurrent response is an indication of the production of hydrogen. Somorjai *et al.* [12,13] have reported that they obtained hydrogen and photocurrent when illuminating the surface of a *p/n* diode with *p*-type photosemiconductor in aqueous solution. However, this method was less effective, as it produced a low yield of hydrogen and a low quantum efficiency. In this study, the photosemiconductive electrodes were made from polycrystalline thin films of sintered Fe_2O_3 doped with MgO or CaO and GaAs. The surface of the photoelectrode was characterized by X-ray diffraction and scanning electron microscopy. Its electrochemical properties were investigated by cyclic voltammetry.

2. Experiments

2.1 Reagents

GaAs was obtained from Korea Electronics and Telecommunications Research Institute and α-Fe_2O_3(Baker GR), NaOH(Junsei GR), MgO (Mallinckerodt GR), CaO(Kanto GR), etc. were used as purchased.

2.2 Instruments

Siemens model D500 X-ray diffractometer (monochromated CuKα radiation) and Siemens model X-650 scanning electron microscope were used for microanalysis of the surfaces. Cyclic voltammetry and were performed with a PAR model 173 Potentiostat/Galvanostat (EG&G) which was equipped with PAR model 175 Universal Programmer and PAR Model 124A Lock-in amplifier(EG&G). 300W tungsten halogen lamp (General Electric) was focused through a quartz tube filled with water and onto the surface of the semiconductor.(*Fig. 1*) All potential values are measured against a Ag/AgCl reference electrode and then scaled to the normal hydrogen electrode.

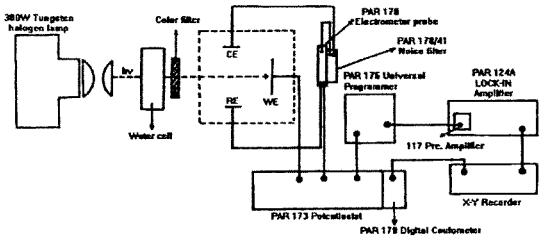

Fig. 1. Experimental equipments for measuring photoelectrochemical properties of a working electrode

2.3 Preparation of doped Fe_2O_3 Photosemiconductive Electrode

Magnesium oxide and calcium oxide were selected from several dopants due to their P-type inclination. Approximately 0.1~15 wt% magnesium oxide or calcium oxide were ground with powder-state iron oxide in an agate morter. The mixed powder was suspended in nitric acid and sprayed onto the Pt foil(spray nozzle diameter: 0.2mm) 20 times over a 3 minute period. During this thick film formation, the temperature of the Pt-foil was held at 300℃ in vacuum(3.5kg/cm^2). This films were then oxidized and sintered in an electric

furnace(Honeywell DCP-7700) at 1,100~1,450℃ over 12 hours, and quenched instantly in the distilled water.

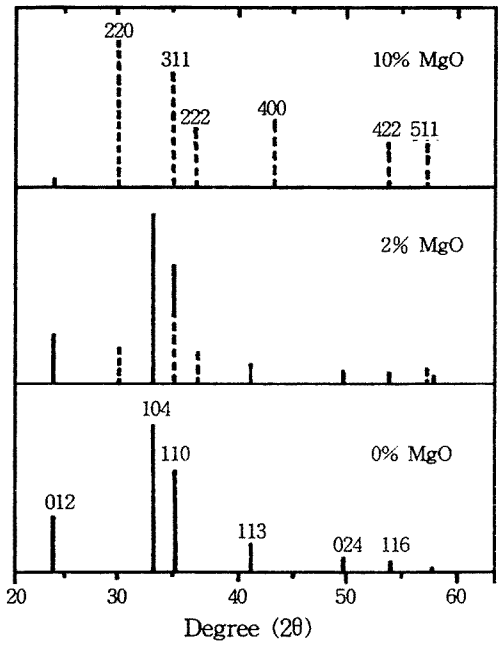

Fig. 2. Schematic X-ray diffraction patterns (CuK α) for MgO doped Fe_2O_3; ——, full line is corundum structure; ·····, broken line is spinel structure.

3. Results and Discussion

3.1 Structure of Magnesium Oxide doped Iron Oxide

The x-ray diffraction pattern for a magnesium oxide-doped iron oxide electrode quenched immediately after sintering at 1,100~1,400℃ exhibited both hexagonal structured corundum of α-Fe_2O_3 and spinal structured Fe_3O_4 or $MgFe_2O_4$. It is known that the spinel structure is mostly formed analogous to $MgFe_{3-x}O_4$ and is affected by MgO dopant amount. This pattern was reported by Dickman *et. al.* [14] The dopant-dependent conversion from the α-Fe_2O_3 corundum to Fe_3O_4 spinel structure above 1,375℃ is displayed in *Fig. 2.* A surface photograph obtained by scanning electron microscopy for the electrode surface of 8.0 wt. % magnesium oxide-doped iron oxide is seen in *Fig. 3.* The comparatively large grain structures of about 1 ~5㎛ are partly compacted on the surface.

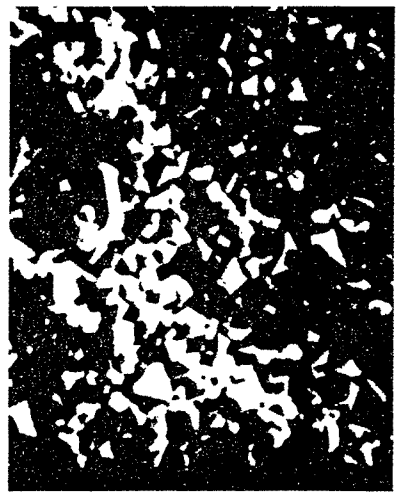

Fig. 3. Scanning electron micrographs of 8.0 wt.% MgO doped Fe_2O_3 thin film.

3.2 Structure of Calcium oxide doped Iron oxide

Fig. 4 shows the scanning electron micrograph of calcium oxide doped iron oxide with dopant amount ranging from 7.0 wt. % to 13.0 wt. %. All samples were rapidly quenched after sintering at 1,100~1,450℃. From this figure, it can be seen that the surfaces are not largely different from each other in grain structure, but the case of 11.0 wt. % dopant has a smaller and thicker layer than that of 8.0 wt. % in grain size. It is also seen that the grain structure is not even and there are many partial cracks in the surface of 7.0 wt. %. These results allowed creation of a model for photocurrent response of the MgO and CaO-doped iron oxides, which involved the presence of two phases, e.g. a bulk corundum (α-Fe_2O_3) and surface spinel phase ($Fe_{3-x}Mg_xO_4$). It can be assumed that a gradient was formed at the interface between

these two phases due to mismatched electrochemical potentials.

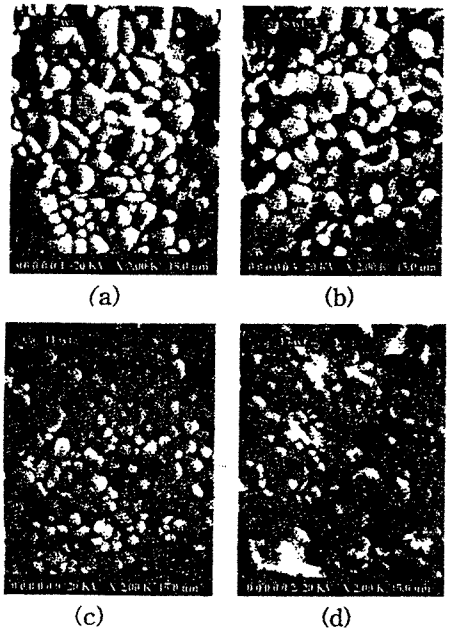

Fig. 4. Scanning electron micrographs of doped Fe_2O_3 thin film. a) 7.0 wt. % CaO doped Fe_2O_3; b) 8.0 wt. % CaO doped Fe_2O_3; c) 11.0 wt. % CaO doped Fe_2O_3; d) 13.0 wt. % CaO doped Fe_2O_3

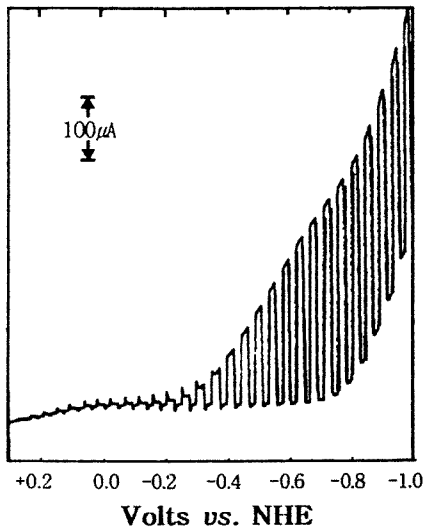

Fig. 5. Cyclovoltammetric photocurrent for the 10.0 wt. % CaO doped Fe_2O_3 thin film electrode; Scan rate 20 mV/sec.

3.3 Photocurrents of CaO doped Fe_2O_3 Photosemiconductive Electrode

Photocurrent of CaO-doped Fe_2O_3 electrode has been obtained by illumination of the surface after biasing +0.5 volts *vs.* NHE in 1.0×10^{-2}M NaOH solution. For a thin film doped with 10.0 wt. % calcium oxide, the photocurrent density was 568 $\mu A/cm^2$ at -0.7 volts *vs.* NHE(*Fig. 5*). Meanwhile, for a film doped with 12.0 wt.%, a typical p-type current density of 527 $\mu A/cm^2$ was shown in *Fig. 6.*

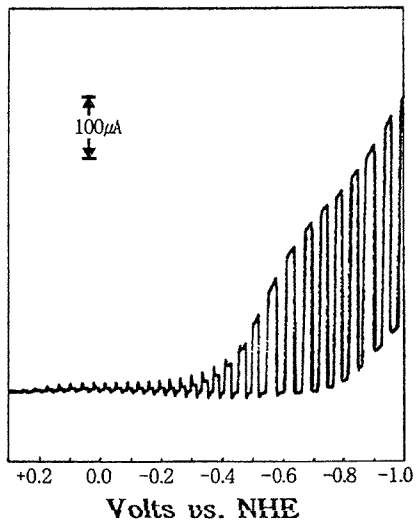

Fig. 6. Cyclovoltammetric photocurrent for the 12.0 wt. % CaO doped Fe_2O_3 thin film electrode; Scan rate 20 mV/sec.

3.4 Photocurrents of MgO doped Fe_2O_3 Photosemiconductive Electrode

The changes in photocurrents of thin film electrodes according to dopant amount of magnesium oxide are shown in *Fig. 7.* The maximum current density of 120 $\mu A/cm^2$ at -0.6 volts indicated that a thin film electrode of Fe_2O_3 doped with 8.0 wt. % magnesium oxide is the best sample for a photocathode in photodissociation.

3.5 Photocurrents of GaAs Photosemiconductive Electrodes and Effect of

Methylene violet

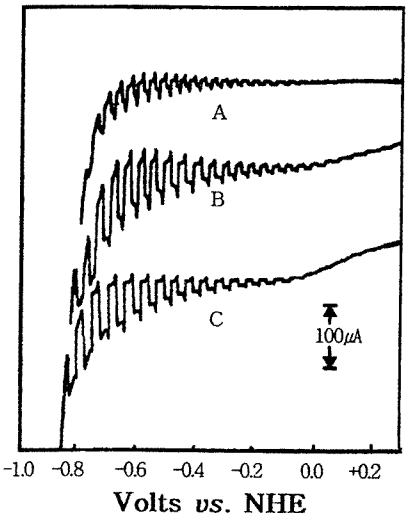

Fig. 7. Cyclovoltammetric photocurrent for the MgO doped Fe_2O_3 thin film electrode.
A: 7.0 wt. % MgO doped; B: 8.0 wt. % MgO doped; C: 9.0 wt.% MgO doped; Scan rate 20 mV/sec.

A GaAs electrode was produced by contacting kanthal wire to the backside of the GaAs wafer with silver epoxy, and photocurrent was obtained after adsorbing 1.0×10^{-3}M methylene violet(MV^{2+}), a known photocatalytic agent, on the electrode surface. The case of pure GaAs is shown in *Fig. 8.* This time, photoanodic current was shown 582 $\mu A/cm^2$ at +0.1 volts as typical n-type response. For the case of adsorbing methylene violet, the n-type photocurrent increased to 1,084 $\mu A/cm^2$ at +0.1 volts but changed to the p-type photocurrent after 8 hours as shown *Fig. 9.* Observing *Fig. 9*, it can be seen that MV^{2+} acted as a photocatalyst. Thus methylene violet adsorbed GaAs seems useful as photocathodic catalyst in the case of the photodissociation of water.

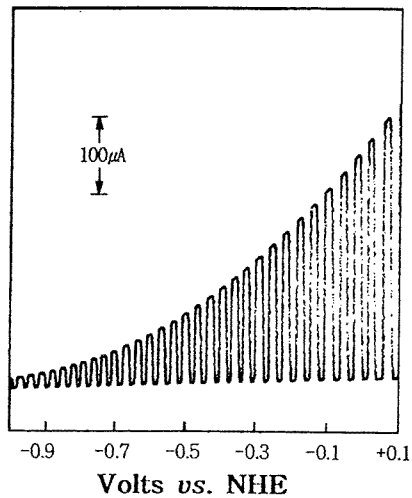

Fig. 8. Cyclovoltammetric photocurrent for bare GaAs in 1.0×10^{-2}M NaOH solution; Scan rate 20 mV/sec.

Conclusions

The preparation and characteristics of magnesium substituted iron oxide ceramics have been examined. It was found that the sintering of cold pressed thin films made from MgO, CaO and Fe_2O_3 powders at temperatures between 1,300 and 1,400 ℃ resulted in heterogeneous ceramic materials containing both α-Fe_2O_3 and a spinel phase, most likely of composition $Fe_{3-x}Mg_xO_4$. While this electrode is consistent with all characterization to perform photoreduction of water, hydrogen evolution will be not correlate with observed photocurrent when these materials are illuminated in aqueous solution. There is some possibility that the observed DC photocurrents are due to a photosynthetic process which does not require transport of carriers though the electrode bulk surface. To improve the photocurrent and cathodic photoreduction, there is some possibility that the modification of the electrode surface with a photosensitizer such as methylene violet and/or the development of

p-type photosemiconductive electrodes such as GaAs. Studies are in progress to elucidate the details on photoreduction of carbon dioxide.

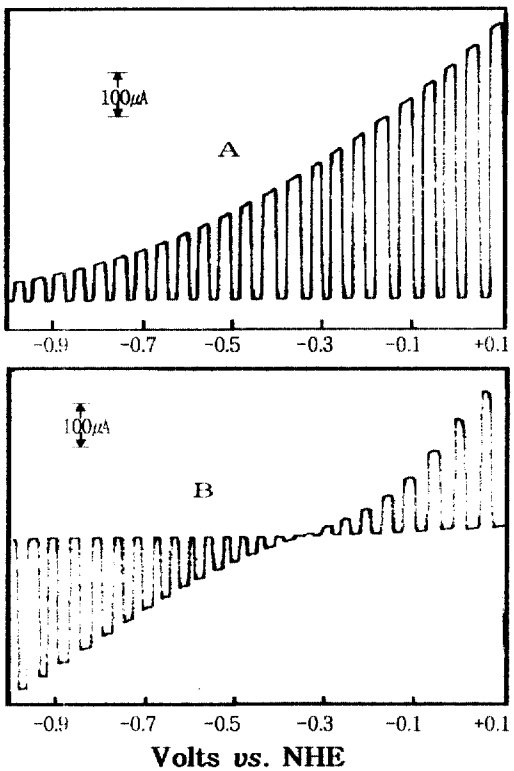

Fig. 9. Photocurrents for methylene violet adsorpted GaAs electrodes.
A : 0.1M methylene-violet adsorpted GaAs in 1.0×10^{-2}M NaOH solution
B : 0.1M methylene-violet adsorpted GaAs in 1.0×10^{-2}M NaOH solution after drying for 8 hours in dry oven.

Acknowledgment

The financial support by the Technology Development on Clean Energy, Ministry of Commerce and Industry are greatly appreciated.

References

1. A. Fujishima and K. Honda, *Bull. Chem. Soc. Jpn.*, 1971, **44**, 1148; *Nature*(London), **238**, 37(1972).
2. H. Gerischer, *Solar Energy Conversion, Topics in Applied Physics*, Vol. 31, B. O. Seraphin, Editor, Springer-Verlag, Berlin 1979.
3. J. H. Kennedy, R. Shinar and J. P. Ziegler, *J. Electrochem. Soc.*, 127(10), 2307(1980).
4. H. L. Sanchez, H. Steinfink, and H. S. White, *J. Solid State Chem.*, **41**, 90(1982).
5. C. Kittle, *Introduction to Solid State Physics*, p.276, John Wiley and Sons, New York, 1953.
6. D. S. Ginley and M. A. Butler, *J. Appl. Phys.*, **48**, 2019(1977).
7. R. Shinar and J. H. Kennedy, *Solar Energy Mat.*, **1**, 237(1979).
8. I. T. Liou, C. Y. Yang, and S. N. Levine, *J. Electrochem. Soc.*, **129**, 342(1983).
9. H. Yoneyama, H. Sakamoto and H. Tamura, *Electrochem. Acta*, **20**, 341(1975).
10. R. F. Gardner, F. Sweett, and D. W. Tanner, *J. Phys. Chem. Solids*, **24**, 1183(**1963**).
11. Y. Matsumoto, M. Omae, K. Sugiyama, and E. Sato, *J. Phys. Chem.*, **91**, 577(1987).
12. C. H. Leygraf, M. Hendewerk, G. A. Somorjai, *J. Catal.*, **78**, 341(1982).
13. J. E. Turner, M. Hendewerk, G. A. Somorjai, *J. Electrochem. Soc.*, **131**, 1779(**1984**).
14. R. Diekman, Ber. Bunsenges, *Phys. Chem.*, **86**, 112(1982).